'Covalent' Effects in 'Ionic' Systems

Paul A. Madden and Mark Wilson
Physical and Theoretical Chemistry Laboratory, Oxford University, South Parks Road, Oxford, UK OX1 3QZ

1 Introduction

How wide is the range of applicability of an *ionic* model of condensed phase structure, energetics and dynamics? The question is posed for practical reasons, as well as for its intrinsic interest. For our purposes, a system which is 'ionic' is one whose properties are reproduced by an interaction model based upon discrete closed-shell ions with integer charges. These ions are not simply charged hard-spheres; they may undergo polarization (induction) and dispersion interactions and may even undergo changes of size and shape ('compression' and 'deformation') due to interactions with their neighbours. What is excluded is charge transfer and chemical bond formation involving the sharing of pairs of electrons between atoms. It is well-known that the domain of applicability of the simplest ionic model, as embodied in Born–Mayer type pair potentials – essentially a model of charged hard-spheres – is severely restricted: even the structure of a material like $MgCl_2$ is not explained despite the large electronegativity difference between the elements involved. Our purpose here is to explore the properties of an *extended* ionic model which allows for *the changes in an ion's properties which are caused by changes in its environment*, and hence incorporate a many body character in the interactions. Among such effects are polarization, compression and deformation. We will show how they may account for many departures from the predictions of the simple ionic model which are conventionally attributed to 'covalency'.

The reason that the question is a practical one is that such an ionic interaction model has two important characteristics. Firstly, it may be used as the basis of tractable computer simulation methods which permit the study of large systems for long times. Such studies are often necessary for an understanding of material properties, and many materials of technical interest lie in the domain where 'covalent' effects are prevalent. The $MgCl_2$ example is the support for the Ziegler–Natta catalyst used in polypropylene synthesis and its crystal surface properties are therefore of interest. More fundamentally, because it is based upon the properties of individual ions, the ionic model is (or should be) *transferable* – it may be used on different phases of the same material, on mixtures and, furthermore, the interaction model for one material should be recognisably related to that of a chemically similar one, by a change in ion size or similar property. A transferable model may be tested on one phase and used on another, tested in the bulk and used for a surface, *etc*. Because of the relationship between materials, the origin of structural trends may be understood and a first guess at an interaction model for one material may be constructed from an established model for another. Born–Haber cycles may be constructed to analyse energetics.

The long-standing difficulty with examining the applicability of the ionic model (including the many-body effects) is that the *individual* ion properties which determine the interionic interactions in condensed phases cannot be determined from experimental data, at least not without further assumptions. However, it is now possible to perform electronic structure calculations to determine the properties of single ions within their condensed phase environment. This breaks the impasse and allows an ionic model to be parameterised unequivocally. Recently, it has been shown how interaction models which allow for an accurate representation of the many-body effects uncovered by such calculations may be constructed and used in tractable computer simulation schemes.[1] The basic physics included in these models is the same as in a (breathing) shell model,[2] the difference being that the shell model[3] makes use of a particular mechanical representation of the many-body effects in order to allow the model's parameters to be determined empirically (effectively, an alternative way of breaking the impasse). However, in so doing it enormously reduces the flexibility available to accurately reproduce the many-body effects, a limitation which becomes clear when comparing with the results of electronic structure calculations of *ionic* properties (such as induced dipoles).[1]

We begin with an account of the origin of the many-body effects, of the way in which they may be characterised in electronic structure calculations, and of their representation in the simulation context. We will then illustrate their role in accounting for various phenomena attributed to 'covalency'. In this we will focus on crystal structure and energetics, since this application provides the most readily appreciated sense of progress, but note that the simulation methods are also applicable to melts and dynamics.

2 Environmental effects and the resulting many-body potentials

To understand the interactions it is not sufficient to think of the condensed phase as a collection of well-defined, gas-phase species. A van der Waals material, such as a rare gas or molecular solid, can be quite accurately modelled this way, but in ionic materials the ions themselves are profoundly influenced by their enviroment. The

Paul Madden is a Professor of Chemistry at Oxford University and a Fellow of Queen's College. He was born in Bradford and obtained his BSc and DPhil at the University of Sussex, the latter supervised by Prof. J. N. Murrell. After a period of eight years at Cambridge, and two at the Royal Signals and Radar Establishment (Malvern) he took up his present position in 1984. He was the recipient of the Tilden Medal of the Royal Society of Chemistry in 1993.

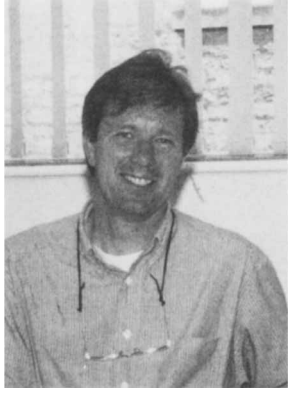

Mark Wilson was born in Derby. He obtained his BA from Keble College, Oxford and his DPhil (supervised by Paul Madden) in 1994. He was then awarded an Alexander von Humboldt Fellowship, which he took up at the Max-Planck Institute in Stuttgart. At the time of publication of this article he becomes a Royal Society Research Fellow in the Physical and Theoretical Chemistry Laboratory at Oxford.

oxide ion, for example, is unstable in the gas-phase but commonly occurs in condensed matter Because of this, the interaction of one ion with another cannot be expressed without reference to the environment in which each ion is found Consequently, interaction potentials must be expected to have an *explicit* many-body character – unlike the van der Waals case, where pair potentials (which may implicitly include the average effects of many-body interac tions) are the norm

To gain more insight into the environmental effects we consider the potential, $V(\mathbf{r})$, experienced by an electron in an ion$^{4-6}$ due to both electrostatic interactions with the charges of the other ions in the crystal and to its exclusion from the region occupied by the electron density of neighbouring ions As illustrated in Figure 1, in a perfect cubic crystal this environmental potential contains a spherical part, $V_0(r)$, plus an angularly dependent potential, which varies rapidly with the orientation of the electronic position $\boldsymbol{r}$ When expressed as a spherical harmonic expansion, this angular part involves terms of angular momentum $l = 4$ or higher, see eqn (2 1)

$$V(\mathbf{r}) = V_0(r) + \sum_{l\geq 4}\sum_{m} V_l(r)Y_{lm}(\mathbf{r}) \qquad (2\ 1)$$

Since the ground electronic state of a closed shell ion is an S state, the angular potential will only be significant to the extent that it can mix in excited states of G symmetry For many ions (especially s–p valence ions) such states are likely to be very far in energy from the ground state, so that only the spherical potential plays any role – the electron density of such ions is unable to adjust to the angularly dependent part of the potential and the electron density of the ion remains spherical The spherical potential, V_0, tends to compress their electron density, relative to that of the free ion, as illustrated in Figure 1 It leads to a marked reduction of the polarizability *inter alia*[4 6] and is responsible for the stability of the oxide ion in condensed matter for cations, the effect is much smaller

2.1 Ion compression in perfect crystals

As the crystal is compressed, there will be an increase in the overlap between the charge densities of nearest neighbour anions and cations, as illustrated in Figure 2 This will lead to an increase in the energy of the system, which we will call U_{ov}, because closed shells may not overlap due to the Pauli exclusion principle If we take electron densities to decay exponentially, and the total overlap energy to be the sum of the overlap energies associated with each cation–anion pair then, referring to Figure 2, the energy would depend on the total hatched areas associated with the overlapping charge clouds We would, therefore, have something like eqn (2 2)

$$U_{ov} = \sum_{i}\sum_{j(\rightarrow i)} A\exp[(r_{ij} - \sigma_i - \sigma_j)/(\rho_i + \rho_j)] \qquad (2\ 2)$$

i e a pair potential of Born–Mayer form, to describe the interionic repulsion Here r_{ij} is the separation between i and j, σ_i is a characteristic radius for the charge density of ion i and ρ_i describes how it falls off with increasing distance from the nucleus To justify this pair potential, we have regarded the ions as fixed entities as the crystal is compressed, so that the extent of overlap increases as in Figure 2(*b*) In general, what should be anticipated is that as the crystal is compressed the walls of the spherical confining potential will move in and each ion will adjust by shrinking its charge density, as illustrated in Figure 2(*c*), where the area of overlap is reduced below what would be found with fixed charge densities Hence, parameters like ρ_i and σ_i, which reflect the size and shape of the charge density, should themselves be regarded as depending on the separation between the ions $\sigma_i \rightarrow \sigma_i(|\boldsymbol{r}^N|)$, *etc* (where $(|\boldsymbol{r}^N|)$ is

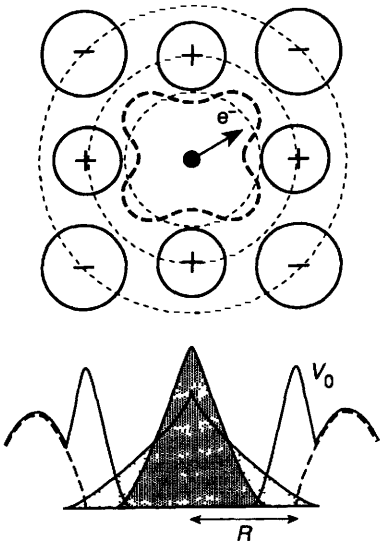

Figure 1 Origin of the spherical confining potential, V_0, which acts on the electrons around an anion in a cubic crystal the electrons in sp valent ions are unable to respond to the rapid angular variation in the potential, illus trated by the dashed contour in the upper panel In the lower panel a cross section through the spherical potential, V_0, is shown the dashed line shows the coulombic (Madelung) contribution, associated with the point ionic charges This is enhanced by the exclusion from the region occupied by the electron density of the other ions V_0 compresses the free anion charge density (lightly shaded) to the in crystal charge density (heavily shaded)

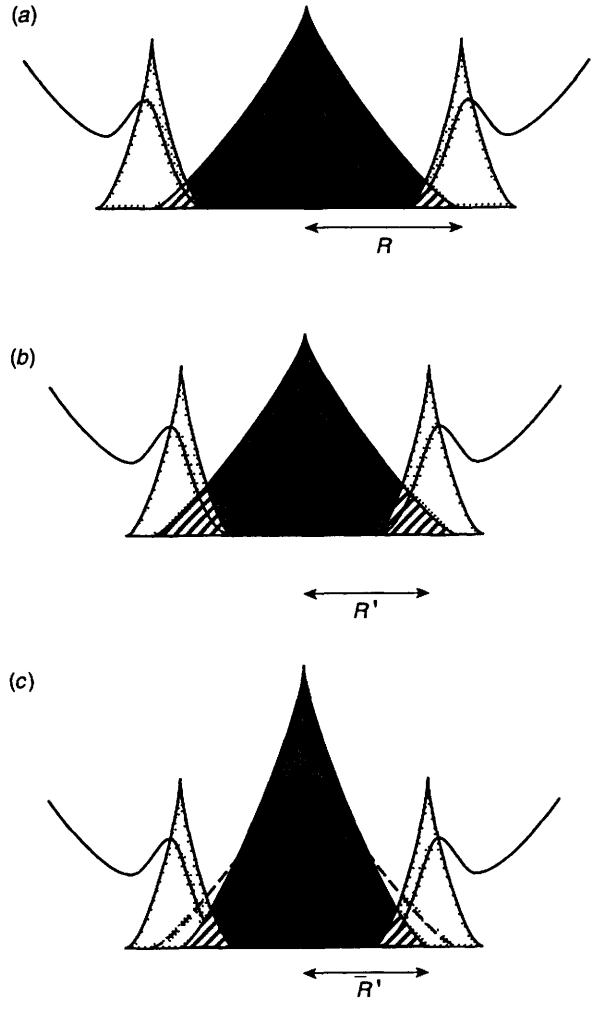

Figure 2 Illustration of the ion compression effect Panel (*a*) shows the anion charge density (dense shading) in the crystal, at lattice spacing R, as confined by V_0 The electron densities of the first cation shell are shown lightly shaded, and the region of cation–anion overlap is hatched After shrinking the crystal (to lattice spacing R') the hatched area increases (*b*) (corresponding to increased repulsion) but the amount of overlap is much reduced [as in (*c*)] if the compression of the anion charge density by the modified confining potential is accounted for The change in shape of the anion charge density gives rise to the self energy U_{self}

intended to imply a dependence on the positions of N other ions in the sample), and the overlap potential acquires a many-body character, eqn (2 3)

$$U_{ov} = \sum_{i} \sum_{j(\neq i)} A \exp[(r_{ij} - \sigma_i[r^N] - \sigma_j[r^N])/(\rho_i[r^N] + \rho_j[r^N])] \quad (2\,3)$$

This shrinkage of the ions under the influence of the confining potential itself costs energy, which might be called a 'self energy', or 'rearrangement energy' – the energy required to place each ion in the confining potential associated with a particular lattice parameter – and the total energy associated with compressing the crystal written as eqn (2 4)

$$U_{rep} = U_{ov} + U_{self} \quad (2\,4)$$

This observation provides a well-defined and practical route for examining the interactions *appropriate to ions in the cubic crystal* The electronic wavefunctions of an anion and cation confined by the *spherical* potentials, V_0, appropriate to the crystal of interest at a particular lattice constant, R, is calculated [4 5 7] The difference between the energy of this confined ion and the free one gives the self-energy appropriate to lattice constant R The interaction between pairs of these entities is then calculated, without further wavefunction relaxation In this way a pair overlap induced-repulsion potential appropriate to R is obtained Such calculations have been carried out by Pyper[5] and his results for U_{ov} and U_{self} for an oxide ion in MgO are shown in Figure 3 [7] Results for the MgO in the six-coordinate rocksalt (B1), the eight-coordinate caesium chloride (B2) and four-coordinate blende (B3) structures as a function of the lattice parameter, R, are shown For the oxide ion the self-energy goes to a plateau at large R this is because the free oxide ion is unstable with respect to O^- plus a free electron, so that, for the oxide ion, we must consider the process of placing an O ion and an electron in the confining potential, rather than simply a free ion The plateau, therefore, reflects the electron affinity of O [5] Note that the self energy is a large component of the total repulsive potential, which resists the compression of the crystal

Why should we worry about separating the total repulsive energy in this way? After all, the total repulsive energy for, say, the B1 phase could still be fitted to a sum of pair potentials by dividing the total repulsive energy involving cations and anions, $U_{ov} + U_{self}$, amongst the six nearest-neighbour pairs The problem is that this representation would not *transfer* to ionic environments other than the perfect rocksalt structure Figure 3 shows that U_{ov} and U_{self} have *different dependencies on coordination number* so that a pair potential calculated with the B1 data would be different from that required to fit the B2 or B3 results Hence, this pair potential would not be *transferable* between the different phases of MgO Pair potentials appropriate to each phase, obtained from the corresponding values of $U_{ov} + U_{self}$, are shown in the inset to Figure 3 and clearly differ However, a compressible ion model (CIM), which allows for the dependence of the σ values on the coordinates of other ions, can be fitted to the data for the rocksalt structure It accurately *predicts* the *ab initio* data for U_{ov} and U_{self} in the other structures,[7] as shown by the solid lines in Figure 3 This model can be used in tractable simulations in place of the pair potential For details, the reader should refer to ref 7 The same physical effect of ion compression has traditionally been accounted for in breathing shell models,[2] but these are normally parameterised empirically

For halide ions U_{self} is found to make a smaller contribution to the total U_{rep} than is the case for oxides[8] (reflecting the greater sensitivity of the oxide ion to environmental effects) Hence for halides, we can anticipate that pair potentials will have a wider domain of applicability than is the case for oxides, which is consistent with the finding that crystal-parameterised Born–Mayer pair potentials were found to give a good representation of the interactions in alkali halide melts *inter alia* [9]

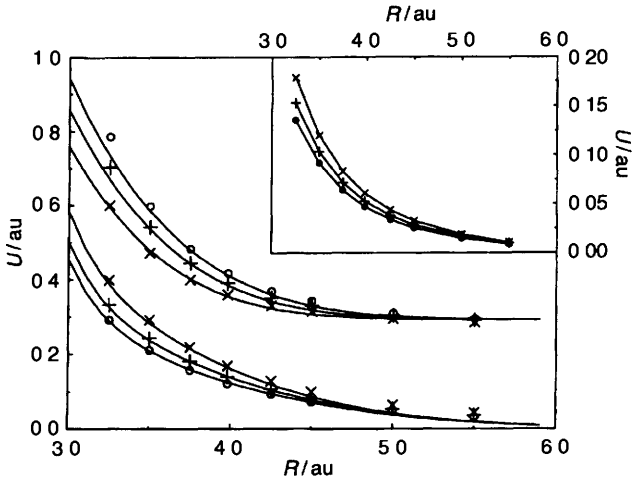

Figure 3 *Ab initio* data for the self energy of an oxide ion (upper family of curves) and for the overlap energy (lower), as a function of the lattice parameter R in four (B3, crosses), six (B1, plusses) and eight coordinate (B2, circles) structures for MgO, as calculated by Pyper [9] The inset shows the pair potentials calculated from this data for each structure, note that these exhibit a coordination number dependence The solid lines in the main figure show the values calculated from the CIM potential [7] which was fit to the B1 data

2.2 Less symmetrical environments

The perfect crystal provides a good reference point for the discussion of environmental effects – an ion in a melt is much more like the in-crystal ion than a gas phase one Nevertheless, to adequately model melts and surfaces a consideration of environmental effects in much less symmetrical environments than the crystal is required A convenient starting point is to consider how the perfect crystal picture, illustrated in Figure 1, is modified when some of the neighbouring ions are shifted off their lattice sites The spherical harmonic expansion of the environmental potential will now, in general, contain angular momentum $l = 1, 2$ components as well as having a modified spherical term As long as the argument – that high angular momentum electronic states are very remote and hence unimportant – remains valid, it will be sufficient to consider the effect of the altered $l = 0$, 1, and 2 potentials The $l = 0$ amounts to a change in the spherical confining potential we discussed above, and may result in a change in ion size The $l = 1$, and 2 terms cause deformations of the ionic electron density of dipolar and quadrupolar symmetry, respectively These may have two consequences Firstly, the central ion will acquire a non-zero electric dipole and quadrupole moment, which will alter its energy through coulombic interactions with the charges and multipoles of other ions this is the polarization energy [10] Secondly, the ion may become non spherical ('deformed') as perceived through the short range overlap interactions with its near neighbours

2 2 1 *Polarization effects*

Polarization effects can be characterized by examining directly, using electronic structure methods, the induced multipoles on ions in distorted crystals There are some technical problems, associated with assigning the displaced charge to a particular ion, but these may be overcome [11]

If an ion in the crystal at a relatively large distance (say, greater than next-nearest neighbour separation) from the central ion is displaced off its lattice site, its effect on the potential felt by the electrons in the central ion is simply that of the electric field ($l = 1$) and field-gradient ($l = 2$) at that site There will be induced dipoles and quadrupoles given by the usual multipole expansion,[10] eqn (2 5)

$$\mu_\alpha^{i\,a} = \alpha_{\alpha\beta} E_\beta(\boldsymbol{r}) + \frac{1}{3} B_{\alpha\beta\,\gamma\delta} E_\beta(\boldsymbol{r})\, E_{\gamma\delta}(\boldsymbol{r}) + \quad (2\,5)$$

$$\theta_{\alpha\beta}^{i\,as} = \frac{1}{2} B_{\alpha\beta\,\gamma\delta} E_\gamma(\boldsymbol{r})\, E_\delta(\boldsymbol{r}) + C_{\alpha\beta\gamma\delta} E_{\gamma\delta}(\boldsymbol{r}) +$$

where the superscript 'as' means that these moments are appropriate when the sources of the fields are *asymptotically* far away from ion i Here, $\boldsymbol{\alpha}$ and $\boldsymbol{C}$ are the dipole and quadrupole polarizabilities

and $\boldsymbol{B}$ is the dipole–dipole–quadrupole hyperpolarizability the components of $\boldsymbol{\alpha}$, $\boldsymbol{C}$ and $\boldsymbol{B}$ are specified by a single number for a spherical ion [10] These polarizabilities are those *appropriate to the ion in its crystalline environment* and, as already remarked, may be much smaller than the free-ion values[6] due to the confinement effects E_α and $E_{\alpha\beta}$ are components of the field and field gradient, respectively

If a near-neighbouring ion is displaced, there is an additional effect Figure 4 shows what happens to the confining potential around an anion, familiar from Figure 1, when one of the first shell of cations is displaced outwards Besides the field and field gradient (related to the gradient and curvature of the potential at the origin) a dent appears in the confining potential Whilst the field and field gradient tend to push the electrons in one direction (away from the displaced cation), this 'dent-in-the-wall'[11] allows them more freedom to move into the space vacated by the cation Hence, there is a short-range contribution to the induced dipole, $\mu^{i\,sr}$, which opposes the 'asymptotic' dipole caused by the electric fields This has been studied in electronic structure calculations The effect is substantial The dipole induced by displacing first neighbour cations is reduced below that expected from the asymptotic term alone by *ca* 50% For induced quadrupoles the effect is even larger the limited evidence available suggests that the short-range term is as large as the asymptotic one, so that the net quadrupole on the anion can be very small or even opposite in sign to the asymptotic quadrupole

In principle, the experimental manifestation of these two effects could be studied in the far-infrared spectra of disordered ionic systems So far as we know, this has not been done quantitatively However, analogous effects contribute to the polarizability fluctuations responsible for light scattering and good agreement has been demonstrated between calculated[12] and experimental spectra [13]

Normally, we think of the anion as the polarizable entity in ionic systems, however, in some cases cation polarization can also become important For cation polarization, the relative sign of the short-range and asymptotic moments is the same – the short-range effect therefore *enhances* the dipoles and quadrupoles above the values which would be expected from the coulombically induced moments If we consider Figure 4 but reverse the signs of the charges on the ions, so as to make the central ion a cation, we can see why As a neighbouring anion is displaced outwards, the electric field generated will tend to displace the cation electrons *towards* the displaced anion which is also the direction favoured by the displacement of the cation charge cloud Again this consideration is true of the higher order multipoles *It makes the role of cation polarization much more substantial than would be suggested by a simple consideration of the relative size of the cation and anion polarizabilities*

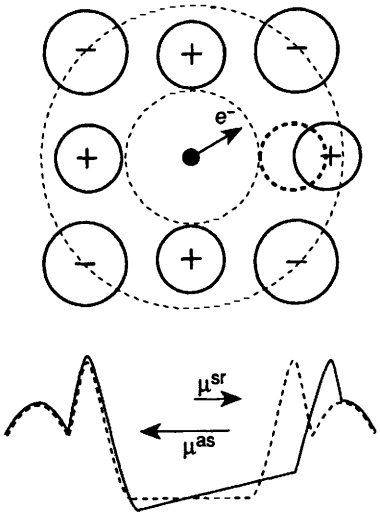

Figure 4 Origin of the 'asymptotic' and 'short range' contributions to the dipole induced in an anion in a crystal which has been distorted by an outward displacement of one of the first shell cations A cross section of the confining potential is shown for the undistorted crystal (dashed), and after the distortion where the 'floor' of the potential well has acquired a gradient (the electric field) and the wall of the confining potential has been pushed outwards These have opposite effects on the electron density Note, the arrows represent the direction of the electron displacement and therefore, strictly, are antiparallel to the associated dipoles

2 2 2 *Deformation of ionic shape*

The development of the multipoles in the less symmetrical structures is a signal that the ion's charge cloud has been distorted from a spherical shape The polarization energy results from the classical coulombic interaction of the multipoles with the charges and multipoles of other ions The deformation of the spherical charge density will also have another manifestation, since it will affect its overlap with the charge densities of the neighbouring ions, and hence it will charge the short-range repulsive interaction with them

This effect is contained within the shell model of the interionic interactions The shell is the centre of repulsive interactions and it may be displaced from the ion's centre of mass (and the site of its formal charge) by repulsive interaction – hence, the ion may become anisotropic [3] A potential difficulty with this approach is that this same displacement is closely tied, in the shell model, to the short-range effect on the induced electric dipole, which was discussed above Although these phenomena are clearly linked we believe, on the basis of a limited set of *ab initio* results, that the connection imposed by the shell model is overly restrictive and that to accurately represent them, the short-range induced dipole and the consequence of the non-spherical deformation on the short-range repulsion should be treated as separate phenomena

This may be done by generalising the treatment of compressible ions indicated in section 2 1 Compression was treated by allowing the ionic radius to depend on the relative position of a number of other ions To allow for a deformation of dipole symmetry, a vector property of each ion $\boldsymbol{\xi}^i[\boldsymbol{r}^N]$ is introduced, which again depends upon the positions of the other ions in the sample, as illustrated in Figure 5 The overlap energy is now given by eqn (2 6)[14]

$$U_{ov} = \sum_i \sum_{j(\rightarrow i)} A \exp[(r_{ij} - \sigma_i[\boldsymbol{r}^N] - \sigma_j[\boldsymbol{r}^N] - \boldsymbol{r}^{ij}\,\boldsymbol{\xi}^i[\boldsymbol{r}^N])/(\rho_i[\boldsymbol{r}^N] + \rho_j[\boldsymbol{r}^N])] \quad (2\,6)$$

The overlap energy between a particular pair of ions now depends not just on the distance between them, but also on the angle between the inter-ion vector and the internal vector $\boldsymbol{\xi}$ of each of the ions, and hence on the configuration of the other ions around i If an ion j is positioned such that $\boldsymbol{r}^{ij}$ is parallel to $\boldsymbol{\xi}^i$, *i e* corresponding to the displaced cation in Figure 5, its repulsive interaction with i is calculated as if the latter's charge density has expanded (enhanced σ^i) $\boldsymbol{\xi}^i[\boldsymbol{r}^N]$ is also associated with a charge in the self-energy of an ion

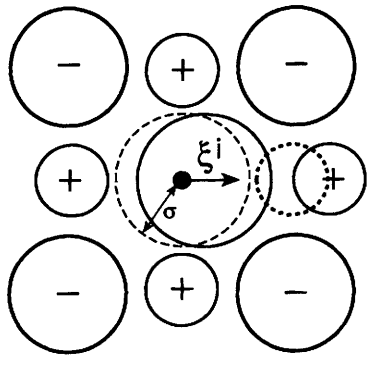

Figure 5 Representation of the ion 'deformation effect' in the distorted crystal considered in Figure 4, the electron density ceases to be symmetrically disposed about the anion centre – as indicated by the displaced contours in the figure This affects the repulsive interaction between the anion and its first neighbour cations The vector ξ indicates the direction of the deformation and appears in the modified expression for the repulsive interactions, eqn (2 6)

A further refinement would be to include a quadrupolar set of internal degrees of freedom to allow for the flattening, or squashing, of an ion

This deformable ion effect may be studied in the same *ab initio* calculations on distorted crystals used to study the induced multipoles Whilst the induced multipoles are obtained directly from the *charge distribution* of the distorted crystals the ion deformation effect is studied *via* the *energies* of these distortions – less the energy which is accounted for by polarization effects

2.3 Representation of the many-body effects

The effects described above give a many-body character to the interionic interactions This arises because the expressions for the interaction energy of a particular pair of ions now contain variables $\sigma^i[r^N]$, $\mu^i[r^N]$, $\xi^i[r^N]$ *etc* , which themselves depend on the coordinates of other particles If we were to express the interaction energy solely in terms of the ionic positions, we would find that it involved very complicated expressions containing the coordinates of different ions *simultaneously* The key to representing the many-body effects in computer simulations is to treat the extra variables,$\sigma^i[r^N]$, $\mu^i[r^N]$, $\xi^i[r^N]$, as dynamical coordinates of the system, wholly analogous to the positions of the ions, and update them, along with the ionic coordinates, as the ions move In terms of the particle positions *and* the additional degrees of freedom the interaction energies become a relatively simple function, involving the positions and additional degrees of freedom of only pairs of ions For details of how this is done in practice, we refer to refs 1 and 7

As described above, we can use electronic structure calculations on compressed and distorted crystals to examine how the ion radius, *etc* vary with the ionic environment We can use these calculations to determine suitable functions, which allow these properties to be evaluated for an arbitrary ionic configuration These functions then become the input to the simulation procedure The hope is that these functions, determined from the crystal calculations, will be sufficiently robust as to allow the properties to be calculated in the more general environments which will be encountered in the melt, at a crystalline defect, *etc*

3 Manifestations of the many-body effects

Many-body effects, such as those introduced above, may affect all aspects of the observable behaviour of ionic systems and influence the properties of melts as well as crystals In order to keep things finite, we will focus primarily on the role of these effects in stabilizing particular crystal structures As we have stressed, the input for the potential models is derived from calculations done on crystalline environments so that the first step of validating a potential must be to demonstrate that it reproduces and explains observed crystalline behaviour Surveys of the structures of binary materials show that, in almost all cases, the local structures of the crystal and melt are closely related [15 16]

The backcloth to the rationalization of crystal structures is provided by the simple ionic model, effectively a model of charged hard-spheres, as embodied in pair potentials of Born–Mayer form For such a model, the most stable crystal structure can be understood by considering how spheres of appropriate charge and radius may pack together to maximize unlike ion coulombic interactions and minimize like interactions [17] These considerations lead to the prediction of a number of typical 'ionic' crystal structures In systems of stoichiometry MX these are the eight-coordinate caesium chloride (B2), six-coordinate rocksalt (B1) and four-coordinate blende (B3) or wurtzite (B4) structures, which are formed in systems of successively lower cation/anion radius ratio The rocksalt (B1) structure, for example, may be viewed as a close-packed cubic lattice of one species with the other occupying the octahedral holes, this arrangement equalises the nearest-neighbour cation–cation and anion–anion separations, $r_{++} = r_{--}$ and hence minimizes the charge–charge interaction For MX_2 systems the corresponding sequence is fluorite (eight-coordinate cations), rutile (six-) and ideal crystabolite (four-) Again, these crystal structures involve ions symmetrically disposed in such a way as to maximise the separation between the more highly charged cations These crystal structures are illustrated in Figure 6

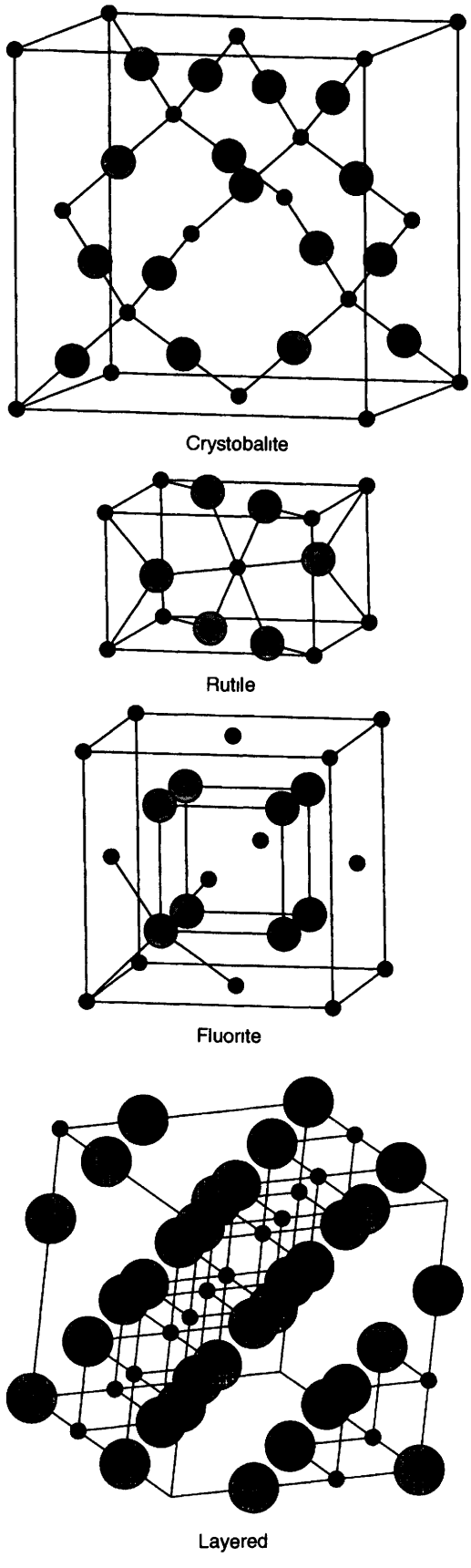

Figure 6 Illustrations of crystal structures frequently adopted by MX_2 systems the small dark spheres are the cations and the larger pale spheres the anions The fluorite, rutile and ideal β crystabolite structures are 'ionic', whereas the CdI_2 is typical of the layered crystal structures, which involve next neighbour anions and a short cation–cation separation

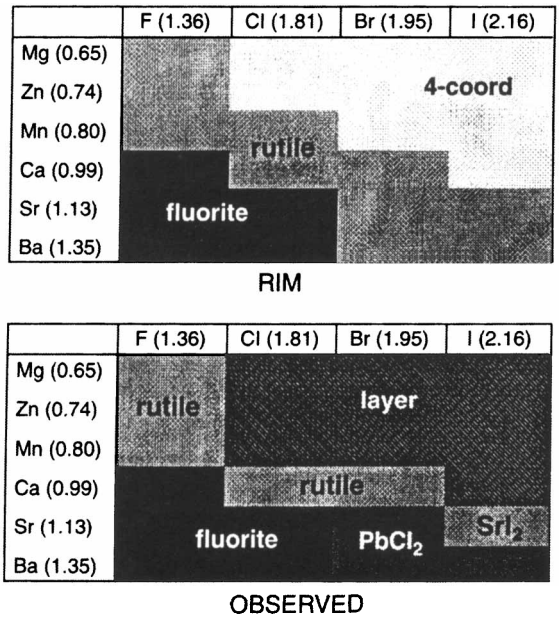

Figure 7 Structure maps, as calculated for alkaline earth halides on the basis of a simple Born–Mayer pair potential (upper), and as observed. Note the agreement in the bottom left corner (large cations/small anions) and the prevalence of layered crystals in the small cation–large anion limit.

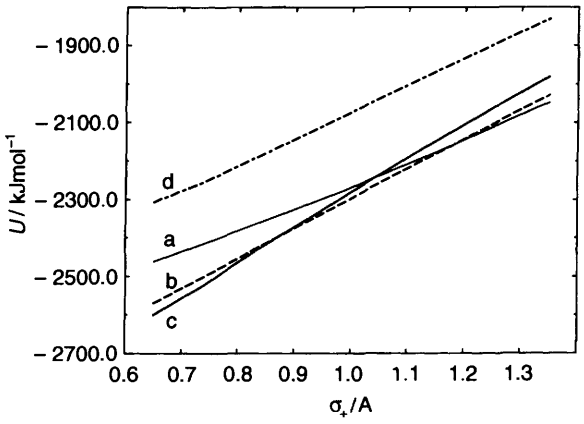

Figure 8 The three lower lines show energies calculated for the various MCl_2 crystal structures from a simple pair potential supplemented with an account of anion polarization, showing agreement with the experimental structural trend 7 (a – fluorite; b – rutile; c – layered). In the absence of the polarization term, the fluorite and rutile energies are barely shifted, whilst the energy of the layered structure is significantly increased (d).

Departures from the simple ionic model may be recognised, qualitatively, in the adoption of crystal structures which do not fit into this pattern. In MX systems, SnO has a layered structure with nearest neighbour ions of like charge along certain directions. In ZnO the ions are tetrahedrally coordinated, whereas the radius ratio would suggest a rocksalt structure. Such departures are much more common in MX_2 or MX_3 systems. This is related to the excess of both octahedral and tetrahedral holes in the close-packed anion structures over the number of cations available to fill them in this stoichiometry – the cations have a much wider range of choice as to how they will organise themselves in the anion lattice than in MX. 'Non-ionic' structures, where the cation occupancy does not minimise the cation–cation interactions, are prevalent. For example, in MX_2 stoichiometry, many systems with small cations crystallize in layered CdI_2 or $CdCl_2$ structures[17] which contain such non-ionic features as nearest neighbour anions, see Figure 6.

In the following sections we will show how, by allowing for environmental effects on the ionic properties, these (and other) anomalies may be rationalized.

3.1 The role of polarization effects

3.1.1 Layered crystals in MX_2 systems

Figure 7 shows that the crystal structures of the alkaline earth halides depart quite markedly from the simple ionic model, despite the large electronegativity differences between the elements involved. Figure 7 contrasts the structure map of stable crystal structures predicted by the simple ionic model, which depends primarily on the radius ratio, with those actually observed for these systems. It shows that whilst the structures adopted by the large cation – small anion systems are as predicted, there is a large portion of the structure map where 'non-ionic' layered crystals are formed, whilst the simple ionic model predicts the crystabolite structure. For reference, the various structures are illustrated in Figure 6. Note that the 'ionic' structures maximize the distance between the highly charged cations and interpose an anion in between a pair of cations, whereas the layered CdI_2 structure contains nearest-neighbour ions of like charge, short cation–cation separations (*i.e.* $r_{--} = r_{++}$, despite the higher cation charge).

For the halide ion, electronic structure calculations reveal that the ion compressibility effects are quite small (compared to oxides, for example); *i.e.* that the total repulsive energy is dominated by the overlap term. The alkaline earth cations are not very polarizable (compared to the chloride ion) and very similar in the gas and condensed phase. Consequently, to a first approximation, we might restrict the consideration of environmental effects to the polarization of the halide ion and use a simple pair potential for the remaining interactions. If we consider a given column of the structure map, *i.e.* a series of systems with the same anion, and impose a very transferable ionic picture on the nature of the interactions, then we would anticipate that the only potential parameter that should vary from one system to another is the cation radius.[18] Figure 8 shows the energy minima calculated[19] for the different chloride crystal structures with a family of interaction models, consisting of Born–Mayer pair potentials with formal ionic charges, supplemented with a description of the halide dipole polarization, which uses an *ab initio* calculated value for the chloride ion polarizability in the condensed phase, and a description of the short-range dipole also derived from *ab initio* calculations. In this family, the only parameter which varies from one system to another is the cation radius; the anion parameters are conserved from one substance to another and the parameters describing the cations are linked in a well defined and chemically meaningful way.

Further calculations show (Figure 8) that the polarization effects have lowered the energy of the layered crystal structures, relative to what would be expected from the pair potential alone, by a huge amount – *ca.* 500 kJ mol^{-1} for $MgCl_2$ – whereas they cause little change in the energies of the 'ionic' fluorite, rutile and crystabolite structures. Figure 6 shows why this has occurred. In the layered crystals the planes of highly polarizable anions are unsymmetrically sandwiched between a plane of cations and anions and are thus strongly polarized in such a way that the negative ends of their induced dipoles are dragged down into the layer of cations. This negative charge 'screens' the repulsion between the positive cations and, therefore, reduces the unfavourable coulombic energy which results from placing them in such close proximity in the layered crystal. In the ideal ionic structures, by contrast, the anions sit in sites of such high symmetry that no dipoles are introduced and the energies calculated with the polarizable model are very close to those obtained with the simple pair potential. Molecular dynamics simulations with the polarizable model confirm that the CdI_2 structure is indeed the globally stable structure for $MgCl_2$.[19]

We therefore see a general pattern emerging:- the simple ionic model favours highly symmetric structures, whereas polarization favours pushing highly polarizable ions into unsymmetrical sites.

Another manifestation of this occurs in the structures of MX_2 melts. A snapshot of the structure in a $ZnCl_2$ melt,[20] simulated with a potential model of the same type as discussed above, is shown in

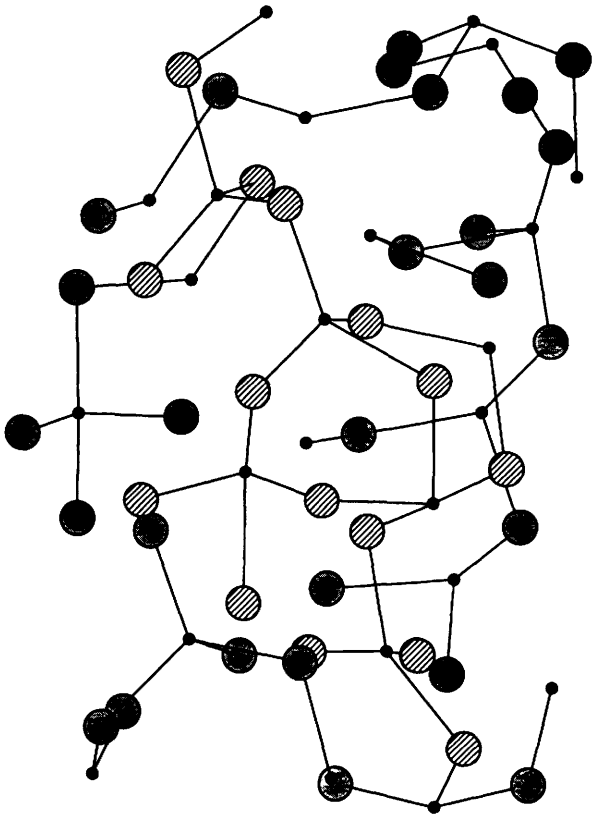

Figure 9 Snapshot of the ionic positions in a simulation of a $ZnCl_2$ melt with a polarizable ion model Cations are small and dark and the anions are larger and more lightly shaded Note the predominant tetrahedral coordination and the corner sharing of tetrahedra involving a bent Zn–Cl–Zn bridge The extent of the network is limited by the fact that 'bands' to Cl ions not inside the region visualised are omitted

Figure 9 It can be seen that the local structure consists of a tetrahedral arrangement of Cl^- ions around each Zn^{2+}, this is an ion size effect, contained within the pair potential, and is a property of the structures obtained when the polarization effects are included or omitted The polarization effects influence the way these tetrahedral units are linked Whereas the pair potential predicts linear Zn–Cl–Zn bridges, on average, the polarizable model gives a bent 'bond' with a bond angle of *ca* 110° Figure 10 shows that polarization is the driving force for the occurrence of this non-trivial bond angle, a phenomenon often attributed to 'covalency' If the bond were linear, the Cl would be symmetrically located between two cations and no induced dipole could result If, on the other hand, the Cl is displaced off the line of centres of the cations a dipole is induced, which serves to screen the cation repulsion and lowers the total energy A more open structure, containing voids, results, so that the price paid for the polarization energy is an increase in the Coulomb, or Madelung energy Numerous observable effects in MX_2 melts may be explained through this phenomenon, in particular, the relationship between like and unlike radial distribution functions,[20] and the 'pre-peak', which is a characteristic feature of network-forming liquids [21]

The specific consequences of the polarization effects depend on a subtle interplay between them, the straightforward coulombic interactions between the ionic charges and excluded volume effects, as determined by the ion size ratio The polarization effects become more important for highly polarizable ions, and when the cation radius is significantly smaller than the anionic one For large cations, the simple ionic structures, with an anion interposed between the cations emerge as most stable At intermediate size, this bridge becomes bent, as illustrated above, resulting in corner linked polyhedra For very small cations and polarizable anions the bending is such as to give edge-linked polyhedra in which the induced dipoles on two anions screen the cation–cation repulsion, as indicated in Figure 10 For example, $BeCl_2$ forms several crystal structures based on chains of edge-linked tetrahedra, and edge-sharing octahedra and tetrahedra become the dominant local structures in MX_3 melts Both of these phenomena are reproduced with potentials of the type described above

3 1 2 Polarization in silica isomorphs

Amongst systems of stoichiometry MX_2, silica (SiO_2) is known to exhibit a particularly exotic range of crystalline isomorphs [17] Whilst there are good reasons to expect that the simple model of a pair potential plus polarization will not suffice for oxides (see below), it is of interest to see how polarization phenomena contribute in these structures, by pushing ahead with the simple model described in the previous section At atmospheric pressure all silica polymorphs are based on corner-linked SiO_4 tetrahedra With increasing pressure there is a transition to a six-coordinate cation rutile-like phase (stishovite) and a possible higher pressure transition to a fluorite-based or α-PbO_2 structure which may have geophysical significance We will discuss results obtained with a Born–Mayer potential with full formal charges, as parameterised by Woodcock, Angell and Cheeseman (WAC), and supplemented by an account of anion polarization, using the oxide polarizability obtained from the experimental refractive index and the short-range dipole function used in MCl_2 work but scaled by the ratio of sums of ionic radii The limitations of this model will become apparent when we consider the relationship between the energies of structures with different coordination numbers

Figure 11 shows the energy/volume curves for the important polymorphs calculated using the WAC pair potential[21] (*a*) without and (*b*) with induced dipoles on the anions In the absence of polarization the lowest energy structures are the ideal-β-crystobalite and tridymite These follow near identical curves (only the ideal-β-crystobalite is shown) as they differ only in the packing of the oxide sublattice ideal-β-crystobalite, as illustrated in Figures 6 and 12, has an fcc oxide lattice whereas the tridymite is hexagonally packed These structures have linear Si–O–Si triplets As discussed above, in the absence of polarization effects the driving force for the linear

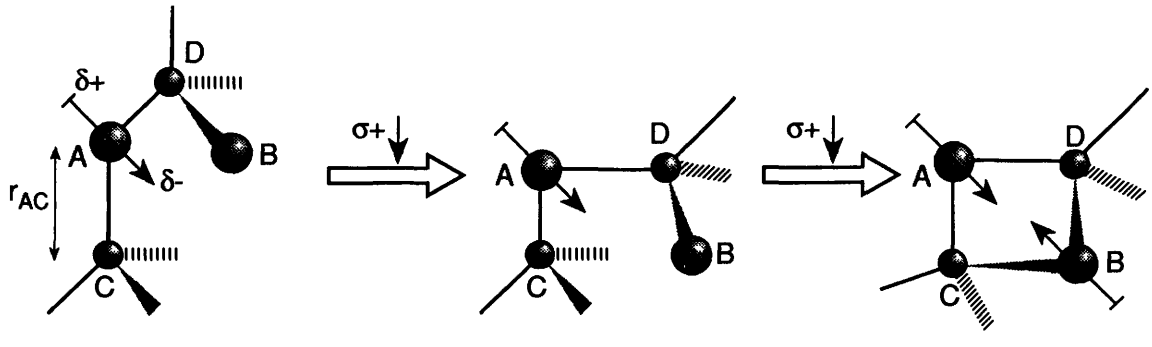

Figure 10 Illustration of the induced dipole as a driving force for bond bending and how, with decreasing cation size (increasing polarization effects), this eventually favours a polyhedral edge sharing motif

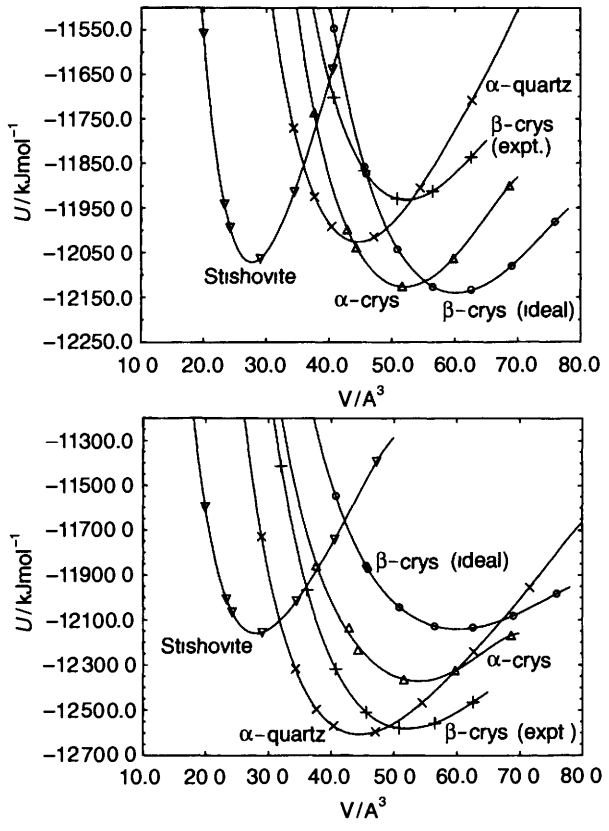

Figure 11 Energy *vs* volume curves for various isomorphs of SiO_2 calculated (*a*) with the simple pair potential[27] and (*b*) with the additional effect of anion polarization Note the stabilization of the experimentally observed β-crystabolite and quartz structures, relative to ideal crystabolite and stishovite, which occurs because of polarization effects

bond is the repulsive cation–cation coulombic interaction which is minimized by interposing an anion between adjacent cations The structures predicted by the pair potential do not agree with experiment ideal crystabolite and tridymite are less stable than the form of crystabolite which is illustrated in Figure 12 and less than the α and β forms of quartz In all these structures the Si–O–Si bond is bent The pair potential also overestimates the stability of the denser, six-coordinate stishovite structure From Figure 12 it can be seen that stishovite is predicted to be stable with respect to both quartz and the experimentally observed form of crystabolite

The inclusion of the polarization effects [Figure 11(*b*)] radically improves this picture Polarization stabilizes the bent Si–O–Si triplets found in the real-crystobalite structures in the same manner as found in the MX_2 systems described above The high symmetries of the oxide sites in the ideal crystabolite, tridymite and stishovite structures preclude such polarization effects The result of allowing for polarization is that the real-crystabolite energy minimum is considerably reduced and now lies significantly below that of the ideal structure and also that of stishovite

The same induction stabilization is seen in the α-quartz structure resulting in the interesting pattern illustrated in Figure 12 Looking down on a plane of SiO_4 tetrahedra, as in Figure 12 (corresponding to the crystallographic *ab* plane) we see alternating up/down spirals of clockwise and anticlockwise induced dipoles which are linked to the piezoelectric properties of quartz

The transition pressure from the α-quartz to stishovite rises to around 50 GPa when polarization effects are included This is a direct result of the greater polarization energy in the four-coordinate structures with respect to the six Although there is some uncertainty as to the actual experimental value, owing to the metastability of the four-coordinate structure, the quoted value (5 5 GPa[22]) is well below our calculated value though the quoted reduction in molar volume on going from quartz to stishovite of 38% is in good accord with the calculations Thus, although the inclusion of polarization effects has qualitatively improved the description of the silica systems it is clear that more is required than adding polarization effects to a pair potential in order to quantitatively account for the phase behaviour Latz and Gordon[23] have argued that the effects of the different environments in these isomorphs on the actual size and shape of the oxide ion must be accounted for to recover the phase transitions accurately, we will discuss such effects in the next section

3.2 The role of compressible-ion effects

So far we have simply examined the consequences of adding polarization to a heuristic pair potential It is unclear whether such shortcomings as the poor quantitative description of the phase behaviour of silica, are due to an inadequacy of the description of

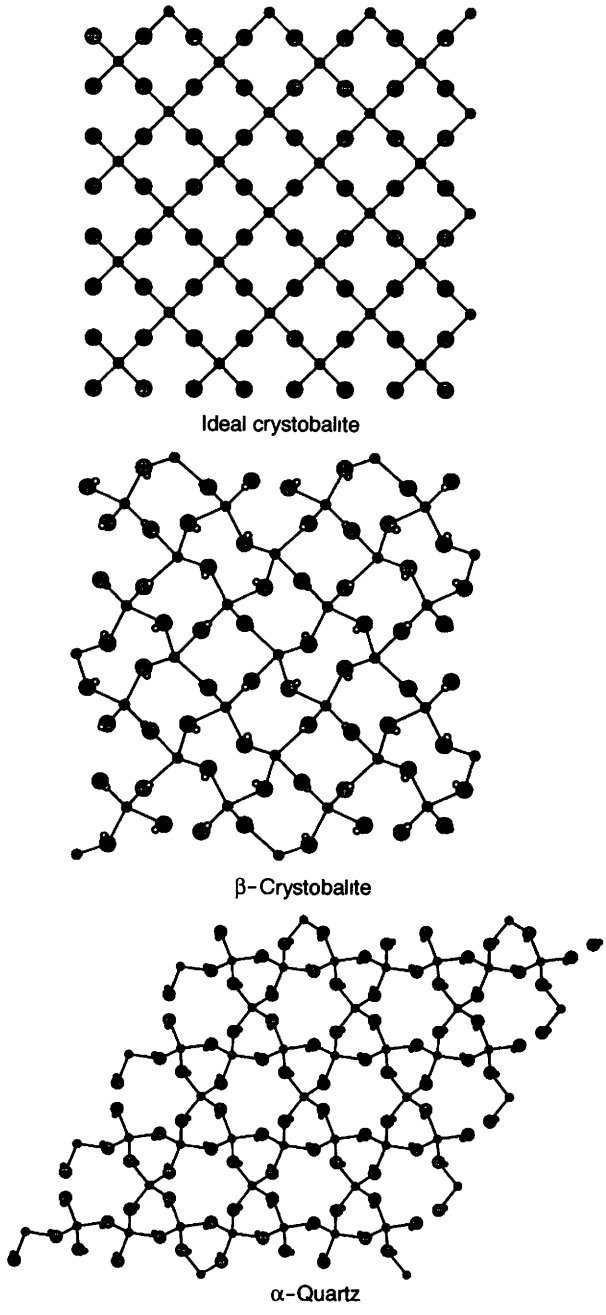

Figure 12 Illustration of the polarization effects in the SiO_2 isomorphs A projection of a single plane of SiO_4 tetrahedra in each structure is shown the Si ions are small dark circles and the O ions are larger and grey The ideal crystabolite (shown in '3D' in Figure 6) is compared with β crystabolite and α-quartz, where the Si–O–Si bond is bent The negative ends of induced dipoles on the oxide ions are indicated by small open circles

the short-range interactions between the ions contained in the pair potential, or due to a more general limitation of the underlying ionic model To proceed further it is clearly necessary to examine the short-range interactions at an *ab initio* level As discussed in section 2 1 such an examination, in cubic crystals, reveals the phenomenon of ion compression We therefore now consider the characteristic effects of generalising the description of short-range repulsion, from that afforded by a pair potential, to allow for the many-body effects which arise from the environmental effects on the ion size

To demonstrate the role of spherical compression, we expand on the MgO example discussed earlier Figure 13 shows the energy/volume curves for the B1, B2 and B3 crystal structures of MgO calculated using (*a*) the compressible-ion model (CIM), discussed above, and (*b*) a pair potential fit to the same rocksalt (B1) data used to parameterise the CIM potential [7] The CIM has been shown to *predict* both the four- and eight-coordinate *ab initio* data also shown in Figure 3 *without further modification* – it is transferable, whereas the pair potential is not (inset to Figure 3) Two features are evident Firstly, the value of the B1 → B2 pressure transition is greatly reduced in the CIM (the transition pressure between the two phases is obtained from the gradient of the line which is a common tangent to the corresponding energy *vs* volume curves) Secondly, and perhaps more strikingly, the predicted ground state for the pair potential is the four-coordinate B3 structure rather than the experimentally observed B1 (rocksalt) The CIM predicts the correct ground state and gives excellent values for its lattice energy, lattice constant and bulk modulus A similar story holds for CaO, for which the B1 → B2 transition pressure is known experimentally and found to be predicted accurately by the CIM potential Thus, allowing for the coordination number dependence of the ion compression effects leads to a transferable potential *which appears to favour high coordination structures* relative to the predictions of a pair potential This appears to be a general observation,

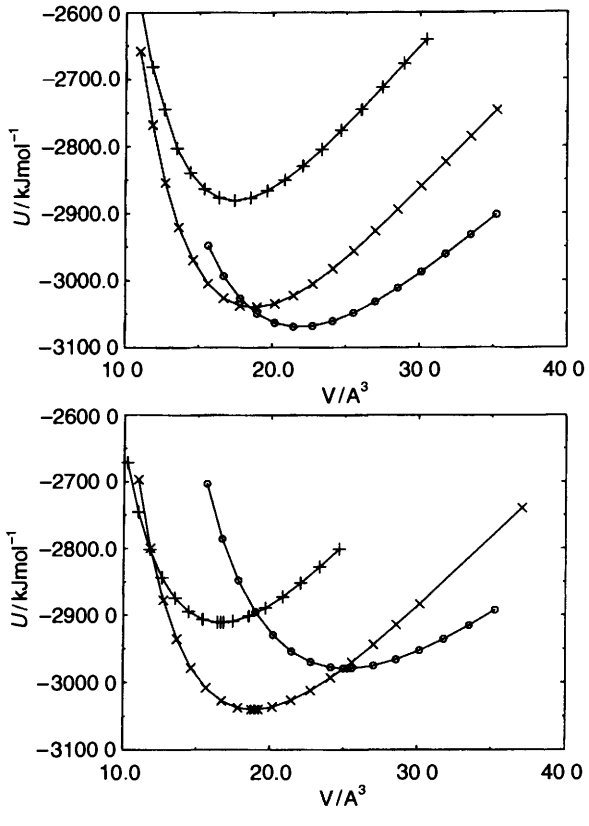

Figure 13 Energy *vs* volume curves for MgO calculated (*a*) with the rock salt pair potential (from the inset to Figure 3) and (*b*) from the CIM potential which represents U_{ou} and U_{self} separately Key plusses – B2, crosses – B1, circles B3 Note that in (*a*) the B3 structure (erroneously) emerges as of lowest energy, whilst the CIM stabilizes the higher coordination structures

for example, a single pair potential with sensible ionic radii cannot reproduce the seven-coordinate ground state of ZrO_2, instead preferring a lower six-coordinate option The use of a CIM corrects this by stabilizing the higher coordinate structure [24] This effect could also help to stabilize the stishovite structure relative to quartz, in SiO_2, and thus improve the predicted transition pressure, as discussed in the last section

How important are the compressibility effects for other anions? The oxide ion, being unstable in the gas-phase, is particularly susceptible to environmental effects *Ab initio* data are available for CsCl and for CaF_2[8] and indicate that U_{self} is a smaller component of the total repulsive energy than in the oxides Nevertheless, Pyper[8] has shown that a full account of the coordination number dependence of U_{ov} and U_{self} is necessary to obtain the correct ground-state (B2) structure for CsCl When the same *ab initio* data are used to fit a pair potential, this potential overestimates the stability of the lower coordination number B1 structure For the fluoride ion in CaF_2, it does seem that a pair potential representation of the repulsive interactions is sufficient [25] The transition energies from the ground-state fluorite structure to a denser α-$PbCl_2$ structure predicted by CIM and pair potential fit to the same *ab initio* data differ by only 8 kJ mol^{-1} in a total lattice energy of *ca* 2500 kJ mol^{-1}, and both are in good agreement with experiment The *ab initio* pair potential (plus polarization) gives a good account of numerous other properties of CaF_2, including its superionicity

In the Introduction, we stressed that one of the touchstones for assessing the validity of an ionic model should be the transferability of the potential Not only should the potential work in different phases of the same material but similar potentials, in which *the parameters change in a chemically reasonable way*, should describe other, chemically related, materials The CIM potentials for MgO and CaO are evaluated from specialised electronic structure calculations which focus on the properties of single ions within an idealised representation of the crystalline environment Nevertheless, the *ab initio* potentials which describe the short-range repulsion between an Mg^{2+} and O^{2-} ion look very similar to those which describe the Ca^{2+} – O^{2-} interaction, if they are scaled to allow for the different radii of the Mg^{2+} and Ca^{2+} ions Furthermore, these potentials may be 'transmuted'[26] into potentials for other oxides of stoichiometry MO simply by replacing the values of well-defined ionic radii in the expression for U_{ov} The self-energy, U_{self} is a property of the oxide ion and should not be changed from one oxide to another It has been shown that these potentials successfully account for the lowest energy crystal structures, energies and lattice parameters of the other alkaline earth oxides and accurately predict the transition pressures to higher density structures Figure 14*a* shows the energy/volume curves for the smallest cation system studied, BeO The observed ground state is now the wurtzite (B4) structure, in line with experiment The energy difference between the B4 and B3 structures is entirely consistent with the slight preference for the B4 indicated by the Madelung constant Figure 14(*b*) shows the same curves for SrO Here, the tangent to the B1 and B2 curves predicts a transition pressure of 27 GPa, which may be compared to an experimental value of 36 GPa

Although the CIM potentials are more complex than pair potentials, they appear to contain an essential aspect to describe phase transitions in oxides but are nonetheless transmutable in a chemically meaningful manner between materials with different cations

3.3 Ion deformation

In order to illustrate the role of aspherical deformation of ions, insofar as these affect the repulsive interactions, we depart from a consideration of crystal structures and consider the lattice vibrational frequencies in MgO How well does the CIM potential, which provides an excellent description of the perfect crystal and its phase transitions, do in predicting the lattice vibrations? As illustrated in Figure 15 the answer is 'very badly!' We know that, since the lattice vibrations involve the movement of ions off their lattice sites, polarization effects must be added to the straight CIM potential and that this will lower the energy of the lattice distortions, and hence

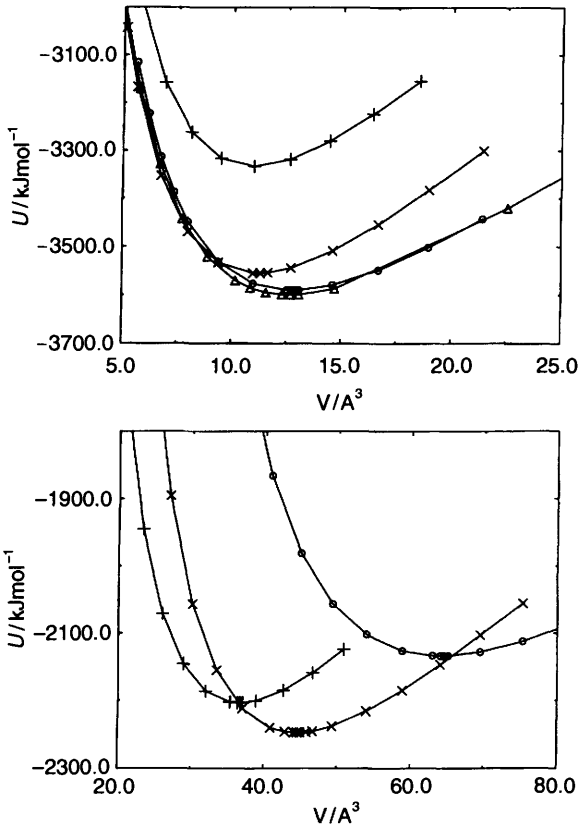

Figure 14 Energy *vs.* volume curves for (*a*) BeO, (*b*) SrO, calculated by scaling the CIM potentials for MgO and CaO to allow for the change in cation radius.[33] Key: plusses – B2; crosses – B1, circles – B3, triangles – B4 (wurtzite). For BeO the wurtzite structure is now (correctly) predicted to be the lowest energy. The B1 → B2 phase transition in SrO is predicted to occur at a pressure of 27 GPa – in reasonable agreement with experiment.

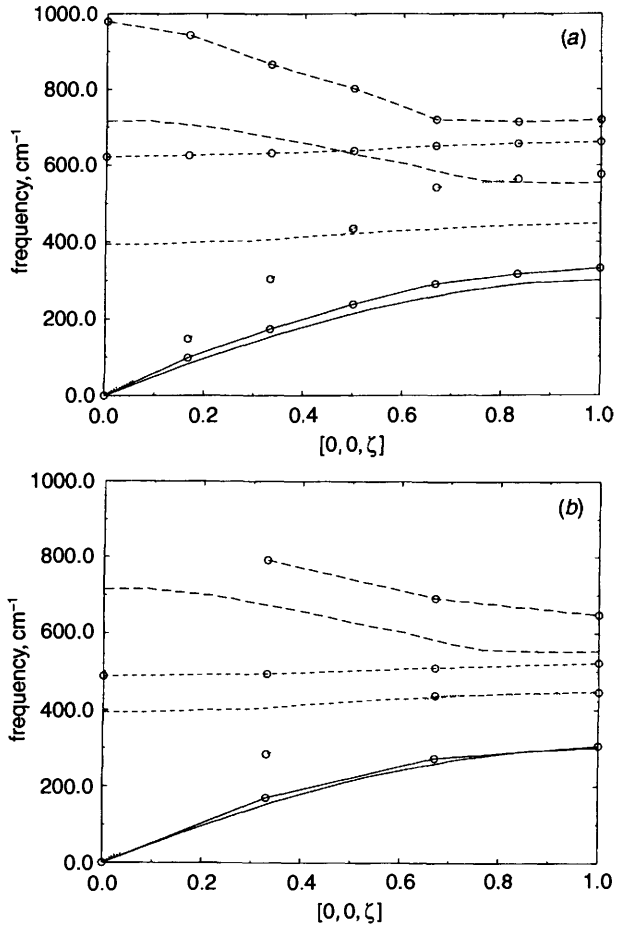

Figure 15 Experimental phonon dispersion curves for MgO[34] along the $k = (00k)$ direction are compared with phonon frequencies calculated (*a*) with the compressible ion potential plus polarization and (*b*) with the additional deformation effect. The type of phonon mode is indicated by the linestyle in both cases (long-dash – LO, short-dash – TO, dots – TA, solid – LA) and the calculated points are indicated by the lines with circles.

reduce the vibrational frequencies. However, the calculated phonon frequencies even when the CIM is supplemented with a description of the oxide ion dipole polarization (*i.e.* with variable ion radius and dipole) are very poor, as shown in Figure 15(*a*). Figure 15(*b*)[14] shows the additional effect of allowing for a deformation of the ion shape of dipolar symmetry [*i.e.* by introducing the variable ξ', as suggested in eqn. (2.6)]. Even when the self-energy associated with the deformation is introduced on an *ad hoc* basis, as was done in these calculations, the shape of the phonon dispersion curves is brought into much better agreement with the experimental ones, although the absolute frequencies of the optic modes is still too high. A better parametrization of this term, and the inclusion of quadrupolar effects is required to obtain the MgO phonons accurately.[14]

4 More complex crystals

In illustrating the characteristic consequences of each of the many-body effects in the last section we have tried to provide examples which draw attention to the role of an individual effect. In the halides, compressibility effects are small and the effects of polarization are clearly seen; in the cubic phases of the alkaline earth oxides, there is no polarization and the compressibility effects are exemplified. We have seen that each of the effects has a characteristic influence on which crystal structure is adopted – polarization favours unsymmetrical sites for highly polarizable ions, neglecting compression leads to an underestimate of the stability of high coordination number structures. In general, the observed structure will be a consequence of competition between opposing tendencies. In this section we consider some more complex examples than those discussed above in which the observed structure reflects this competition.

4.1 Al_2O_3 – higher-order multipoles

The competition between the different effects becomes marked when considering the more complex M_2O_3 stoichiometry, since almost all possible crystal structures for such systems give site symmetries which are capable of sustaining induced multipoles. Attempts to model Al_2O_3 with shell models, which allow for dipole polarization, cannot account for the higher stability of the observed corundum structure over the less dense bixbyite phase unless unreasonably large values for the dispersion interaction between pairs of aluminium ions are included.[28] This artificially stabilizes the close approach of a pair of Al^{3+} ions, a characteristic feature of the corundum structure. In both the bixbyite and corundum structures the oxide ions are fourfold coordinated but, whereas the coordination is almost tetrahedral in bixbyite, in corundum the tetrahedra are twisted towards a planar D_{4h} geometry. Although neither of these site symmetries can support a significant induced dipole moment, in the corundum structure there is an appreciable field gradient at the oxide site which can induce a quadrupole. This suggestion is corroborated by findings from nuclear quadrupole resonance studies[29] of the magnitude of the field gradients at ^{18}O and Al nuclei, which had been used to estimate the magnitudes of induced quadrupoles on the O^{2-} ions and which are consistent with a value for the quadrupole polarizability C of O^{2-} of 5–7 a.u.[30] Apart from supporting different polarization effects, the oxide sites in corundum and bixbyite will lead to different degrees of compression of the oxide ions.

Simulations of Al_2O_3[31] have been carried out with a CIM potential derived from the MgO, by a small change in the cation radius,

and including dipole and quadrupole polarization [using the asymptotic model of eqn (2 5)] A C value of 6 a u predicts the corundum structure to be stable with respect to bixbyite with an energy difference between the structures consistent with results from *ab initio* calculations as well as good structural parameters The dipole polarization plays a very minor role, because of the relatively high symmetries of the oxide site in both lattices

This is not quite the end of this story however In MgO the *ab initio* O^{2-} quadrupole polarizability has a value of 26 a u ,[32] and its value in Al_2O_3 would be expected to be similar (in-crystal oxide polarizabilities are found to depend, largely, on the cation–anion separation, which are very similar in MgO and Al_2O_3) Such a large polarizability would give a much larger value for the energy difference between corundum and bixbyite and would lead to nuclear field gradients considerably larger than those observed in NQR We would interpret this as a good example of the influence of the short range contribution to the induced multipoles, as discussed in section 2 2 1 The effect of these terms is to substantially reduce the induced quadrupoles on anions from the values predicted with the asymptotic model The influence of the short-range terms is mimicked in the calculations by introducing a much reduced value for the quadrupole polarizability

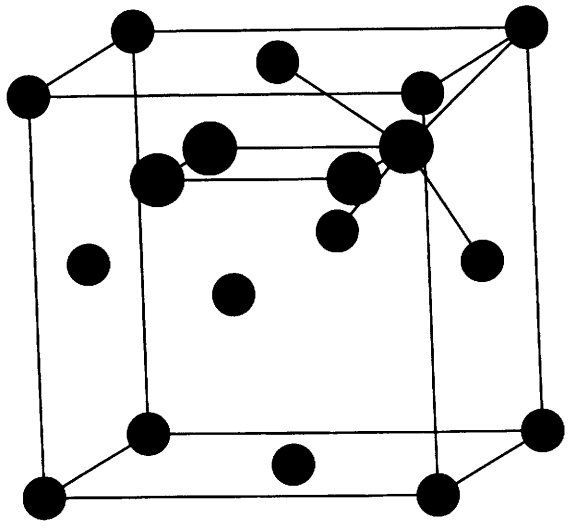

Figure 16 The SnO crystal structure, illustrating the unsymmetrical occupation of the unit cell by oxide ions Cations are the small dark spheres and oxide ions the larger pale ones

4.2 SnO (and PbO) – cation polarization

As described above, a family of CIM potentials can be obtained for the alkaline earth oxides, which differ substantially only in the value of a cation radius, and which quantitatively account for the phase transitions observed in this series between the 'ionic' B2 (CsCl-eight-coordinate), B1 (rocksalt-six-coordinate) and B3/B4 (blende/wurtzite-four-coordinate) crystal structures We might therefore expect to be able to predict the structures of other oxides of stoichiometry MO simply from the cation radius Amongst the exceptions to the general pattern of 'ionic' structures in MO systems is SnO which, together with PbO, crystallizes into the litharge structure shown in Figure 16 [17] In the ideal structure (sketched, the true structure involves a slight distortion) the anions occupy *tetrahedral* holes in a cubic cation lattice, whereas radius considerations would suggest a rocksalt structure, as formed by SrO (σ_{Sn2+} = 1 12 Å compared with σ_{Sr2+} = 1 18 Å[18]), in which the larger octahedral holes are occupied More strikingly, the pattern in which the tetrahedral holes are occupied is different from the four-coordinate cubic blende structure In the latter the occupancy is strictly *charge-ordered*, and $r_{--} = r_{++}$ In the SnO structure, since alternate *planes* of holes are occupied (see Figure 16) $r_{--} = r_{++}/\sqrt{2}$ and nearest-neighbour cations occur an arrangement which clearly does not minimise the charge–charge interactions Further evidence regarding the difference between SnO (and PbO) and the alkaline earth oxides comes from the lattice formation energies,[18] which are more negative than those of the alkaline earth oxides with similar cation radii

The analogy between the SnO structure and the layered crystals formed by MCl_2 systems seems clear There are, however, two important differences Firstly, the greater number of anions in the MX_2 stoichiometry and the greater cation charge lend themselves to the anion–dipole stabilization mechanism – the excess of octahedral holes over cations means that asymmetric structures can arise, even for intermediate size cations Only symmetric structures, which do not allow dipole induction, can arise from occupying octahedral holes in an fcc lattice at MO stoichiometry because of the equal number of ions and holes Secondly, previous examples of such dipolar stabilization have been confined to systems in which it is the *anion* that sits in the asymmetric environment, whereas in SnO it is the cation Simple electronic structure arguments suggest that the dipole polarizability of the Sn^{2+} cation could also be very large Its ground-state configuration is $5s^2$, which means that there are low energy, dipole-allowed transitions (5s → 5p) which could make a very large contribution to the polarizability *Ab initio* results confirm this,[33] with the value of α = 15 a u very similar to that expected for the anion in this system, and much larger than the Sr^{2+} polarizability (5 a u) Calculations show that polarization energies associated with such a large cation polarizability are sufficient to overcome the charge ordering tendency and to drive the O^{2-} ions into the tetrahedral holes in the cubic Sn^{2+} lattice, despite the large cation/anion radius ratio, in such a way as to generate the layered structure which allows the cation polarization

4.3 ZnO – the preference for a tetrahedral site

From the perspective of the alkaline earth oxide CIM, another 'anomaly' may be recognised Zn^{2+} has a slightly larger crystal radius (0 74 Å[18]) than the Mg^{2+} ion (0 68 Å) and yet the lowest energy isomorph of ZnO is the four-coordinate B4 (wurtzite) structure,[17] whilst MgO is rocksalt In the alkaline earth oxides, only the tiny Be^{2+} (0 45 Å[18]) falls in the four-coordinated B4 domain This preference of the Zn^{2+} ion for a tetrahedral site, relative to Mg^{2+}, is general – seen in the crystal structure of the chlorides, for example The application of pressure to ZnO does result in a phase transition to the higher coordinate B1 between 9 0[41] and 9 5 GPa [34] Thus, the energy of the B1 phase is relatively close to that of the B4 in ZnO, whilst the former has a smaller molar volume

Dipole (and quadrupole) polarisation effects, which we have considered previously, cannot contribute to the energetics of these structures because the site symmetry is too high to permit such multipoles to be induced Mahan has noted the potential significance of *octupole*-induction at tetrahedral sites [35] The octupole polarizability, which would control the magnitude of this effect might be large for a post-transition metal ion like Zn^{2+} because of the possibility of octupole-allowed d → p transitions This is confirmed by electronic structure calculations which show that the octupole polarizability, Ω, of Zn^{2+} (*ca* 29 a u) is *ca* 50 times greater than Mg^{2+}, suggesting that cation octupole polarization could be responsible for the different coordination preferences of the two ions

However, the same calculations show that Ω for the O^{2-} ion in these systems should be about 161 a u – so that, if the octupole polarization were simply that driven by the field gradient from the ionic charges (*i e* the asymptotic model of section 2 2) the octupole polarization of the anion would swamp that of the cation, so that any discrimination between Zn^{2+} and Mg^{2+} from this mechanism would be lost Furthermore, were the oxide ion octupole polarization energy obtained with the asymptotic model to be included in the energetic considerations for the alkaline earth oxides, a B3/B4 ground-state structure would be predicted for MgO as well! The item missing from these consideration is the short-range contribution to the polarization As discussed in section 2 2 1, for anions this dramatically reduces higher-order polarization effects, such as oxide octupole induction, but for cations it enhances it Detailed considerations show that the crystal structure of ZnO can be rationalised on the octupole induction mechanism [26]

This finding is a significant one in trying to evaluate the limits of validity of the 'extended' ionic model, at least in a practical sense The starting point of this model, as expounded in section 2 2, is that ions are basically spherical in high symmetry crystal structures and that only distortions of low multipolar order need to be included to account for the changes in their properties as they sample the environments typically encountered in the condensed phase The ZnO finding, however, points to the fact that higher order distortions of post-transition metal cations need to be incorporated even to account for the lowest energy crystal structure – the Zn^{2+} ion is intrinsically aspherical in a condensed phase This certainly poses a challenge for a computationally tractable implementation of the 'extended' ionic model

5 Conclusion

In the article we have described an approach to the representation of interionic interactions in which formal ionic charges are used and in which the many-body effects have been broken down into distinct physical effects which may be *separately characterized* in electronic structure calculations and *separately represented* in tractable computer simulation models We have shown that each of these effects can exert a distinctive influence on condensed phase structures and account for phenomena which have conventionally been regarded as non-ionic (or 'covalent') The potentials have been shown to be transferable, not only between different phases of a given material but 'transmutable' between chemically related systems by substituting parameters with a physically transparent significance We believe that the work has shown that an ionic model, where the ions carry formal charges, has a wider domain of applicability than has sometimes been supposed This has opened the way for more wide-ranging simulation work, with well-founded potentials

We have tended to use the expression 'covalent' in a somewhat pejorative sense, as a catch-all term to 'explain' anything not predicted by the simplest ionic picture Enderby and Barnes[16] describe covalency as 'interactions which change the charge distribution of the valence electrons relative to some conceptual extreme, represented in our case by the ionic model', this seems to sanction the catch-all useage As chemists we would prefer a less catholic use of the term and to retain it for the description of interactions arising from chemical bond formation involving the sharing of pairs of electrons between atoms If we then attempt to find more specific explanations of the most spectacular 'covalent' anomalies (layered crystals, bent 'bonds' *etc*) it would seem that many can be attributed, quantitatively, to *ionic* polarization – covalency, in the chemical sense, is not involved Detailed considerations of the relative energies of different structures necessitate an allowance for the fact that an ion's size and shape may change in different environments, but this may still be encompassed within a fully ionic picture of closed shell species carrying formal charges The invocation of each of these aspects of the 'extended' ionic model in a particular material is driven by a consideration of the electronic structure of the ions involved Thus, the concept of ions as spherical rests on the remoteness of electronic states of high angular momentum the oxide ion is particularly compressible compared to halides, due to its instability in the gas-phase cation polarization becomes especially important when low-energy, dipole-allowed transitions are possible, as in Sn^{2+}

Quite how far this picture can be carried, beyond the examples we have given, at a quantitative level, remains to be seen

Acknowledgements We are grateful to several colleagues for their work and discussions on the topics we have covered, in particular we thank John Harding, Nick Pyper, Adrian Rowley, Nick Wilson and Malcolm Walters We also thank Emily Carter for her comments on the manuscript and John Freeman for help with the figures

References

1 M Wilson and P A Madden, *J Phys Condens Matter* 1993, **5**, 2687, *J Phys Chem*, 1996, **100**, 1227
2 U Schroder, *Sol Stat Commun* , 1966, **4**, 347
3 B G Dick and A W Overhauser, *Phys Rev* , 1958, **112**, 90
4 G D Mahan and K R Subbaswamy, 'Local Density Theory of Polarizability', Plenum, London, 1990
5 N C Pyper, *Adv Sol Stat Chem* , 1991, **2**, 223
6 P W Fowler and P A Madden, *Phys Rev B*, 1984, **29**, 1035
7 M Wilson, P A Madden, N C Pyper and J H Harding, *J Chem Phys* , 1996, **104**, 8068
8 N C Pyper, *J Phys Condens Matter*, 1995, **7**, 9127
9 L V Woodcock and K Singer, *Trans Faraday Soc* , 1971, **67**, 12
10 A D Buckingham, *Adv Chem Phys* , 1967, **12**, 107
11 P W Fowler and P A Madden, *Phys Rev B*, 1985, **31**, 5443
12 P A Madden, *J Chem Phys* , 1991, **94**, 918
13 G N Papatheodorou, and V Dracopoulos, *Chem Phys Lett* , 1995, **241**, 345
14 A Rowley and P A Madden, to be published
15 M Rovere and M P Tosi, *Repts Prog Phys* , 1986, **49**, 1001
16 J E Enderby and A C Barnes, *Repts Prog Phys* , 1990, **53**p, 85
17 U Muller, 'Inorganic Structural Chemistry', Wiley, Chichester, 1993, A F Wells, 'Structural Inorganic Chemistry', fifth edn , Clarendon, Oxford, 1984. R W G Wyckoff, 'Crystal Structures', Interscience, New York, 1965
18 R D Shannon, *Acta Crystallogr Sect A*, 1976, **32**, 751, J G Stark and H G Wallace, 'Chemistry Data Book', 2nd edn John Murray, 1984
19 M Wilson and P A Madden, *J Phys Condens Matter*, 1994, **6**, 159
20 M Wilson and P A Madden, *J Phys Condens Matter* , 1993, **5**, 6833
21 M Wilson and P A Madden, *Phys Rev Lett* , 1994, **72**, 3033
22 R A Robie, B S Hemingway and J R Fisher, *Geol Surv Bull* , 1979, **21**, 1452
23 D J Lacks and R G Gordon, *J Geophys Res* , 1993, **98**, 22147
24 M Wilson, U Schonberger and M W Finnis, *Phys Rev B*, submitted
25 N T Wilson and P A Madden, *J Chem Phys* , submitted for publica tion
26 M Wilson and P A Madden, *Mol Phys* , to be published
27 G Peckham, *Proc Phys Soc* , 1967, **90**, 657
28 J P Gale, C R A Catlow and W C Mackrodt, *Modelling Simul Mater Sci Eng* , 1992, **1**, 73
29 E Brun, E Hundt and H Niebuhr, *Helv Phys Acta* , 1968, **41**, 417
30 S Hafner and M Raymond, *J Chem Phys* , 1968, **49**, 3570
31 M Wilson, Y M Huang, M Exner and M W Finnis, in preparation
32 H M Kelly and P W Fowler, *Mol Phys* , 1993, **80**, 135
33 M Wilson, P A Madden, S A Peebles and P W Fowler, *Mol Phys* , 1996, **88**, 1143
34 J C Jamieson, *Phys Earth Planet Inter* , 1970, **3**, 201, C H Bates, W B White and R Roy, *Science* 1962, **137**, 993
35 G D Mahan, *Sol State Ionics*, 1980, **1**, 29. *Sol State Commun* , 1980, **33**, 797